1 *In vitro* effects on cellular shaping, contratility,
2 cytoskeletal organization and mitochondrial activity
3 in HL1 cells after different sounds stimulation. A
4 qualitative pilot study and a theoretical physical
5 model.

7 **Carlo Dal Lin MD[1°*], Claudia Maria Radu BD, PhD [2,3°], Giuseppe Vitiello[4], Paola Romano[5,6],**
8 **Albino Polcari[7], Sabino Iliceto MD[1], Paolo Simioni MD, PhD[3] and Francesco Tona MD, PhD[1]**

9 [1] Department of Cardiac, Thoracic and Vascular Sciences, University of Padua, Medical School Padua, Italy.
10 [2] Department of Women's and Children's Health, University of Padua, Padua, Italy.
11 [3] Department of Medicine, Thrombotic and Haemorrhagic Diseases Unit, Veneto Region Haemophilia and
12 Thrombophilia Centre, University of Padua Medical School, Padua, Italy.
13 [4] Department of Physics "E.R.Caianiello" Salerno University, Fisciano (Salerno), Italy
14 [5] Dipartment of Sciences and Technologies, Sannio University, Benevento, Italy
15 [6] CNR-SPIN Salerno, Baronissi (Salerno), Italy
16 [7] IISS "Giovanni XXIII", Salerno, Italy

18 * Correspondence: Carlo Dal Lin, MD, Department of Cardiac, Thoracic and Vascular Sciences, Padua
19 University School of Medicine, Via Giustiniani 2, 35100 Padua, Italy. Fax: +39-049 8211802 Phone: +39-049
20 8218642 Email: carlodallin@libero.it

22 ° **Carlo Dal Lin and Claudia Radu equally contributed to this work.**

24 **Abstract:** Convincing evidence has documented that mechanical vibrations profoundly affect the
25 behaviour of different cell types and even the functions of different organs. Pressure waves such as
26 those of sound could affect cytoskeletal molecules with coherent changes in their spatial
27 organization and are conveyed to cellular nucleus via mechanotransduction. HL1 cells were grown
28 and exposed to different sounds. Subsequently, cells were stained for phalloidin, beta-actin,
29 alpha-tubulin, alpha-actinin-1 and MitoTracker® mitochondrial probe. The cells were analyzed with
30 time-lapse and immunofluorescence/confocal microscopy. In this paper, we describe that different
31 sound stimuli seem to influence the growth or death of HL1 cells, resulting in a different
32 mitochondrial localization and expression of cytoskeletal proteins. Since the cellular behaviour
33 seems to correlate with the meaning of the sound used, we speculate that it can be "understood" by
34 the cells by virtue of the different sound waves geometric properties that we have photographed and
35 filmed. A theoretical physical model is proposed to explain our preliminary results.

1. Introduction

There has been vast evidence that shows how cells are able to communicate with each other through light emissions[1,2], electromagnetic signals[3,4],[5] and mechanical / acoustic vibrations[6,7],[8],[9].

In particular, it appears that mechanical vibrations profoundly affect the behavior of different cell types and even the functions of different organs[10,11],[12],[13]. Pressure waves such as those of sound could affect certain cells or their structures determining microvibrations, or even causing resonances, i.e. the synchronization of the biomolecular oscillatory patterns within cells[14].

For example, it has been shown that bacterial cells are able to respond to specific single acoustic frequencies and are able to emit sounds[15].

Moreover, it has been demonstrated that acoustic vibrations in the form of single frequencies[16], noise or music, alter proliferation, viability[17] and hormone binding [18] in human cells cultures and in animal models[19,20],[21].

Ventura et al. have recently reported that human stem cells seem to respond to complex sound frequencies (melodic music, rhythm patterns and human voice) with different electromagnetic emissions measured with a Multi Spectral Imaging system[22].

Furthermore, acoustic stimuli seem to be of paramount importance in guiding the spatial interaction between cells, thus influencing their individual and collective behavior[23],[24].

It is very probable that all this evidence transmits, at a macroscopic level, the phenomena of cellular mechanotransduction, a discipline that focuses on how extracellular physical forces are converted into chemical signals at the cell surface. However, mechanical forces that are exerted on surface-adhesion receptors, such as integrins and cadherins, are also channeled very rapidly along cytoskeletal filaments and concentrated at distant sites in the cytoplasm and nucleus[9,25,26], altering cellular genome activities[27].

All the research conducted so far has mostly explored the possible biological effects of ultrasound or audible acoustic vibrations only in terms of cellular behavior, often using single or very simple frequencies; but what happens inside a living cell exposed to sounds? What could be the molecular effect of music, noise or of the words we hear or pronounce in our everyday life?

Since words and music are a compound of several sound frequencies, and are indeed mechanical vibrations, which can cause mechanical stress, it seems not odd to expect a direct molecular effect in our cells. The present work was thus designed to better understand the direct effects of acoustic vibrations in the form of music, noise and words in cardiac muscle cells *in vitro* culture in their contractility and their tendency to form cytoskeletal cellular networks in space.

Microtubules represent one component of the cytoskeleton and are composed of dimers of alpha e betta tubulin. Microtubules interacts with the other cytoskeletal proteins and it is responsible of the structure, shape of cell and in its movements. Microtubules interacts with other cytoplasmic organelles such as mitochondria and regulates their functions (metabolic energy)[28]. Microtubules system undergo in a rapid polymerization and depolymerization turnover by exchange their subunits (in the order of msec). In cardiac cells the interaction of microtubules system and mitochondrial play an important role in providing the bioenergy needs for the contraction of cardiac cells[29]. As microtubules, actin is involved in a dynamic process of polimerizzation-depolimerizzation. Thus, we focused our attention on these dynamic systems.

We exposed cultures of murine atrial cardiomyocytes (HL1) to 20-minute sound sequences. In particular, as an example of sounds with opposite characteristics, we used some meditative music,

utterance, music with high frequencies, high rhythm and saturated sounds, a collection of urban traffic noises and human screams. A 20 minute repetition of single words: a sound that is repeated during meditation practices, and the sounds "Ti amo", (I love you) and "Ti odio" (I hate you) were also used. These last sounds, as an example of words commonly used, with opposite meanings. We followed the cellular behaviour (contraction, vesicular trafficking, indirect cytoskeletal movements) directly in response to each different acoustic stimuli, acquiring a time lapse video with frames taken every 100 msec. Then, we analyzed any changes of the cytoskeleton by immunofluorescence technique. Finally, in order to explain the results, we also photographed and filmed the geometric characteristics of the waveforms of the sounds used.

2. Results

The HL1 cells were treated with different sounds for 20 min. The experiment was repeated for 6 times with the same outcome. The results were divided into two groups according to the stimulating or inhibiting effect of the sound (Supplements-Figure S2). Below we present the results for the vibration "Ti amo" and "Ti odio" as representative of the two categories (panels B and C of all the figures) compared to those of the control with spontaneous cell's growth without any sound (panels A of all the figures). As depicted in the Figure S1, the other sounds we used produced similar effects. In all the figures, the sounds travel from right to left.

Control cells without any sound treatment portray casual organization of cells and normal expression of the different markers (panel A of all the figures).

HL1 cells were stained for alpha α-tubulin and MitoTracker® (MTr). Following the "Ti amo" sound exposition, the expression of α-tubulin increased drastically and the mitochondrial marker decreased considerably (Fig. 1-B) while after the "Ti odio" sound the cells decreased sharply the expression of the same markers (Fig.1-C). Furthemore, tubulin distribution in Fig. 1-B seems to be organized as a net of filaments perpendicular and parallel to sound waves. In Fig. 1-B we can notice how tubulin forms "bridges" between cardiomyocytes, an important aspect of cell to cell communication and contractility[49]. After the "Ti odio" sound exposition (Fig.1-C), cells show spatial disorganization and their number decreased probably due to its "explosion" (Supplements-movie S1 series).

In Fig 2. HL1 cells were stained with phalloidin (F-actin) and β-actin. The expression of both F-actin and β-actin increased after the "Ti amo" sound, (Fig. 2-B) while the cells decreased the expression of the same markers after the "Ti odio" sound (Fig. 2-C), as confirmed in Table I that describes their mean intensity fluorescence in three different ROI. The augmented expression of these markers in Fig. 2-B may indirectly reveal an increased cell activity and motility[27] as shown in movie S2 series-supplements.

In Fig 3. cells were stained with F-actin and alpha-actinin-1. In controls (Fig.3-A), alpha-actinin-1 localization seems to be more perinuclear. After the "positive" sound exposition, its distribution is more diffused (Fig.3-B) while after the "negative" sound its expression is strongly decreased. We want to highlight the alpha-actinin-1 builds bridges between F-actin filaments[27], which is another aspect that could further explain the increase in cell contractility shown in movie S2 series-Supplements.

Table I quantitatively describes the molecular expression changes according to the sounds used.

Table I. Mean fluorescence intensity of 3 different Regions Of Interest (ROI) taken in 3 different images of the same marker.

	A	B	C
Phalloidin	17.8±4.3 #∗	30.3±5.4 #•	6.1±2.9 ∗•
Beta-actin	1.5±0.3 #∗	7.4±1.9 #•	2.7±0.6 ∗•
Alpha-actinin-1	1.5±0.2 #∗	3.1±0.7 #•	1.0±0.2 ∗•

 # Mann-Whitney for independent samples A vs B p<0.05

∗ Mann-Whitney for independent samples A vs C p<0.05

• Mann-Whitney for independent samples B vs C p<0.05

A= control; B= "Ti amo" sound; C= "Ti odio" sound
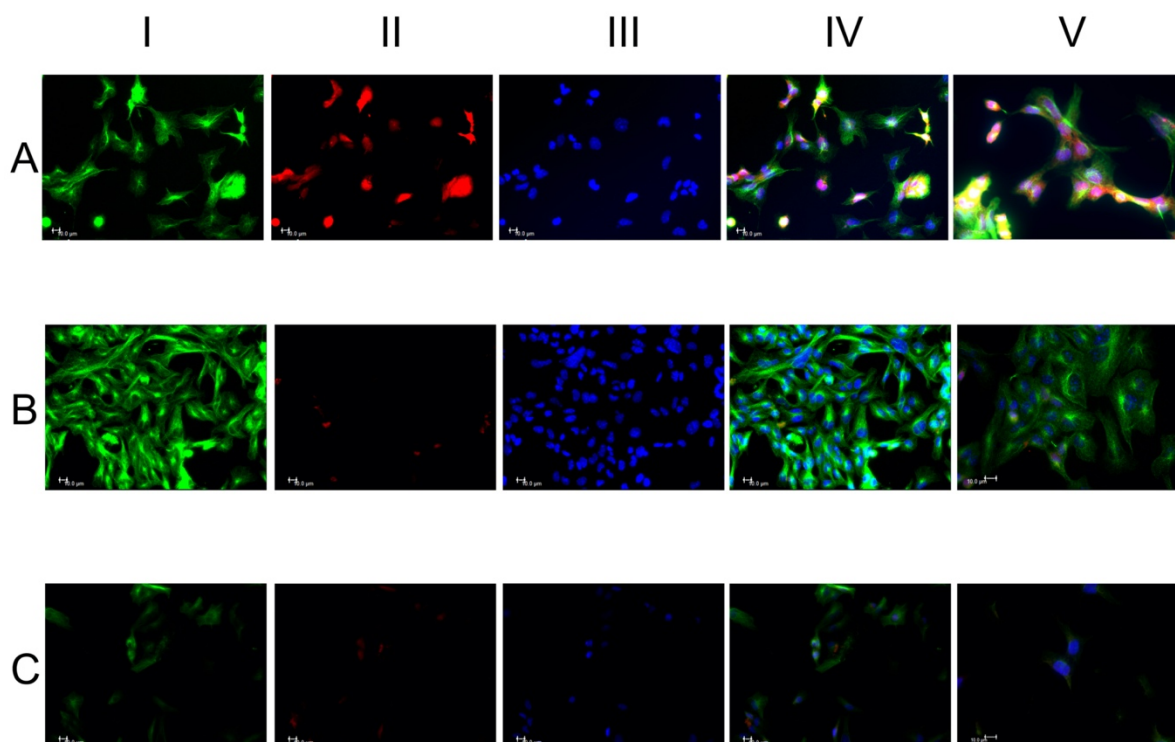
2.2. Figures

Figure 1. Alpha tubulin (α-tubulin) and MitoTracker (MTr) stained after treatment with different sounds for 20 min (representative images). The cells received the sound from right to left. HL1 cells were stained with α-tubulin (green fluorescence) column I, MTr (red fluorescence) column II and the nuclei were stained with Hoechst 33258 (blue fluorescence) column III. Merge of the three fluorescence, column IV. Representative merge fluorescence images at 100x/1.4 oil objective, column V. Panel A, control cells without any sound treatment showing casual organization of cells and normal expression of the different markers. Panel B, the expression of α-tubulin increased and the mitochondrial marker decreased. Cells with more orderly spatial organization with perpendicular tubulin distribution and parallel to sound waves. The nuclei appear with more regular size.

146   Analysis with a greater objective (column V, panel B) highlights the filamentous and granular
147   cytoplasmic expression of tubulin. In the image tubulin forms "bridges" between two
148   cardiomyocytes which is important in the cell to cell communication (asterisk). Panel C, the HL1 cells
149   show a spatial disorganization and the number of cells decreased. Moreover, the different markers
150   expressions markedly decreased. The low number could be due to the "explosion" of cells with
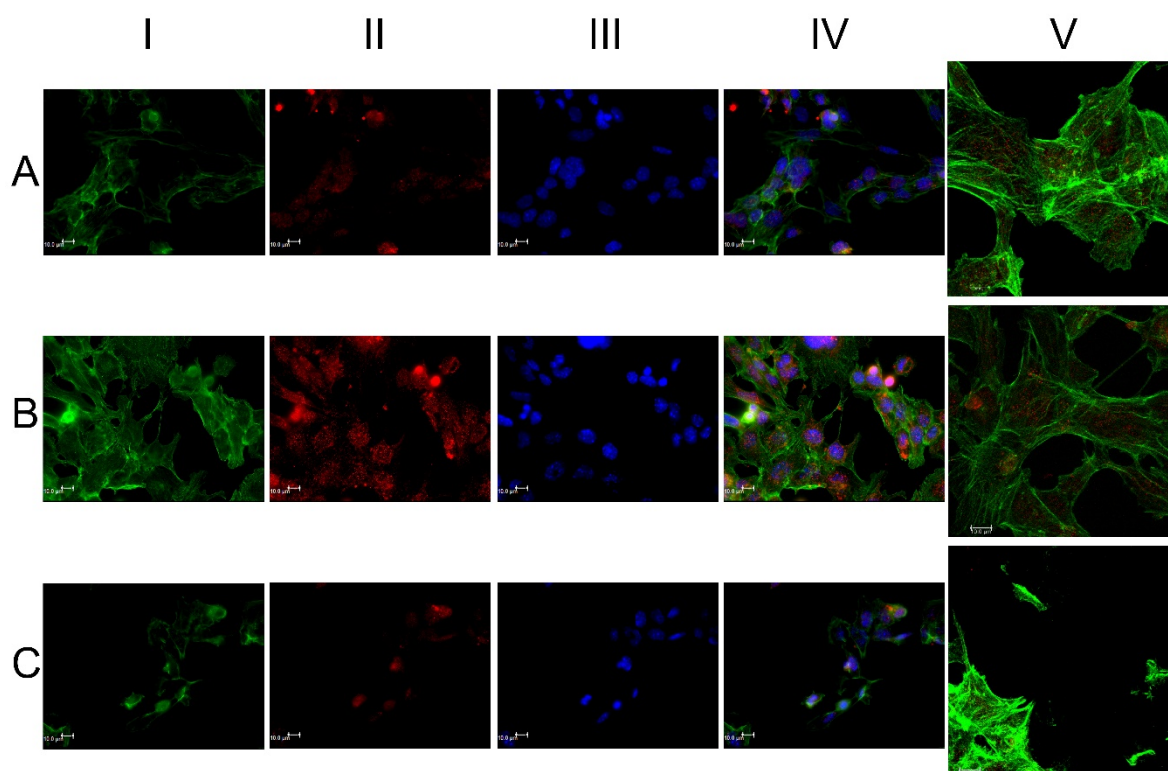151   cytoskeletal fragmentations (asterisks). Scale bar 10μm.

152

Figure 2. HL1 cells were stained with phalloidin 488 conjugated (green fluorescence) column I, β-actin (red fluorescence) column II and DNA with Hoechst 33258 (blue fluorescence) column III. Overlay of the three fluorescence images, column IV. Representative merged images of F-actin and β-actin with confocal microscope (100x/1.4 oil objective), column V. Panel A, control cells without any sound stimulus and normal expression of the different markers. Panel B, increased of both expressions of the two markers. Peripheral and filamentous expression of phalloidin and with a spatial organization as descripted in Fig. 1. Panel C, decreased number of cells with markedly fragmentation of cells (asterisks). Evident reduction of the expression of the different markers. Scale bar 10μm.
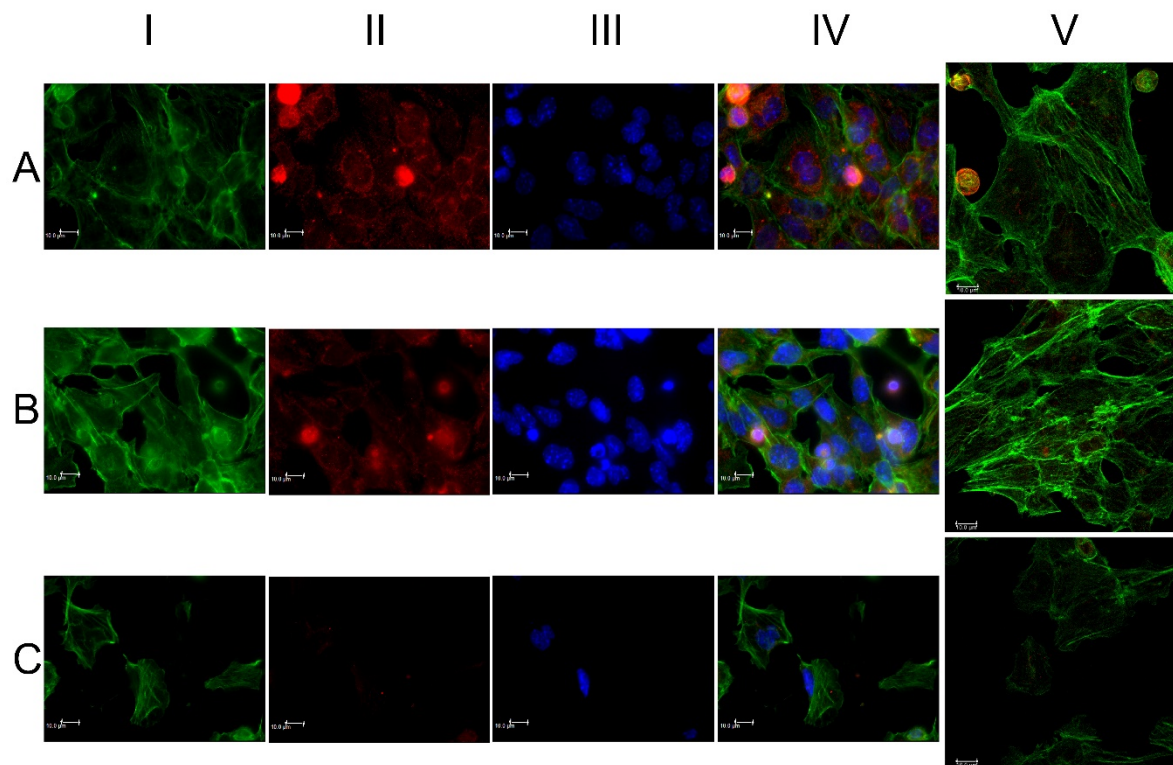
Figure 3. Cells stained with phalloidin and alpha-actinin-1(green and red fluorescence, column I and II, respectively) and DNA stained with Hoechst 33258 (blue fluorescence). Panel A, perinuclear alpha-actinin distributions. Panel B, major cellular organization and diffuse alpha-actinin distribution. Panel C, evident cellular fragmentation with loss of the normal morphology of the cell with nucleus towards the peripheral part (white asterisks). Decrease or absence of markers expression with following loss of cytoskeletal organizations (asterisk orange). Scale bar 10μm.

3. Discussion

Qualification is not quantification. We are describing a proof of concept study and we need to make an important clarification to understand our results: our aim was to document any *qualitative* difference in cell behavior and cytoskeletal characteristics without focusing on *quantitative* assessments that will be the subject of further studies. Every biological phenomenon has qualitative and quantitative aspects of equal and complementary importance. Indeed, a quantitative expression variation of a subcellular component does not inform us about any possible conformational change or of a different spatial localization that could, even with the same quantity, justify a modification of cellular behavior. Any quantitative difference does not constitute a condition neither sufficient nor necessary to explain a biophysical phenomenon or, in our case, the interaction between sound vibrations and *in vitro* cells. We consider more appropriate to integrate quantitative studies with qualitative observations, from which we decided to start replicating them for 6 times.

Our results seem to highlight a different cell growth pattern depending on specific sound stimuli, with a different expression/organizzation of cytoskeleton proteins and mitochondrial activity[28]. The cellular behaviour of HL-1 cells also appears to change as a function of the sound stimulus that impacts on their surface: some biomechanical acoustic stimulations enhance contractility and increase the vesicular traffic within them, while others hinder it, reaching cell lysis. We speculate that this could be related to a transcriptional stimulation effect, based on the observation of Wang et al[27].

188 The present observations and the videos in the supplementary material show how HL-1 cells
189 respond in a highly sensitive fashion to vocal sounds and music or noise with opposite and, in
190 hindsight, "predictable" results based on the type or the meaning of the acoustic stimulus itself.

191 The sounds used in this work are obviously composed of a spectrum of peculiar acoustic
192 frequencies that propagate in a liquid medium (such as the culture medium used) by drawing
193 different geometric shapes (movie S3-supplements) as already demonstrated by Chang et al[30].

194 We assume that the meaning of the sounds we used could be encoded in their specific
195 geometric form, and that the wave trains characteristic of each acoustic vibration can: 1) directly
196 modulate the cytoskeleton morphology[26,31] by penetrating signals of mechanical stress or relaxation
197 up to the nucleus, thus interfering favourably or not with the trafficking of organelles (such as
198 mitochondria[32]), of cellular micro-vesicles[33] and influencing protein oscillatory motions normally
199 present in the cytoplasm[34]; 2) arrange the traffic and the electromagnetic interaction[35],[36] between
200 the molecules dissolved in the cytoplasm, regulating processes crucial to cell survival[37,38] according
201 to the mechanisms exemplified in the supplementary animations (movie S4-supplements). It is not
202 surprising that there may be an intimate relationship between trains of acoustic waves and
203 proteins[37], given that the proteins in the human body vibrate in different patterns like the strings on
204 a violin or the pipes of an organ[39] and may interact with each other even through quantum
205 interference[40].

206 On one hand, it is known that acoustic stimulations deform[41,42] and are conveyed[26,43–46] by the
207 cytoskeleton to the nucleus[27] and on the other, the tubulin monomers exhibit different oscillatory
208 and assembly modes[47] depending on the frequencies that go through them[3]. Furthermore,
209 microtubules seem to be able to capture *phonons*, i.e. "quanta of sounds" or vibrational / mechanical
210 energy packages, within them, energy that would then be used in different cellular processes,
211 including cell division and movement[48]. In addition, it seems that *phonons* play an important role in
212 regulating the structure and stability of a crystalline system[49]: further studies will be needed to
213 extend this consideration to a complex system like a living cell, whose membranes, DNA, proteins
214 and cytoskeleton seem to present analogies with a crystal lattice.

215 We remember that this is only a qualitative pilot study and we specify that the sounds and
216 words used in this work are only an example of possible vibrations that we emit or to which we are
217 exposed every day and of which we wanted to see a possible cellular biomechanical effects. Then,
218 further studies will be needed to evaluate the complex phonological features of different sounds,
219 music and words, pronounced by different people in different languages and cultures. Moreover,
220 our results refer to "Ti amo" and "Ti odio" just as vibrations. Further studies will be needed to
221 establish if the meaning that we assign to a specific sound is only a convention or related to its
222 physical/geometrical mechanical properties.

223 In Appendix-1 we hypothesize a theoretical physical model at the basis of our results which
224 could be very important for future research.

225 It is really intriguing to note that, as well as a scream or sound conveying in a geometric
226 waveforms vibration ("Ti odio") seem to induce cellular stress, as revealed by James Gimzewski
227 with an atomic force microscope[50] that produces a sound of a scream.

228 **4. Materials and Methods**

229 In Supplements-Figure S*1* it's possible to see the laboratory set up for the experiment.

230 *Cell culture.* The murine atrial cardiomyocyte cell line HL1 was obtained from the laboratory of
231 William C. Claycomb (New Orleans, USA). The cells were grown in Claycomb medium

232   supplemented with 10% fetal bovine serum (FBS, cat # F2442), 0.1 mM norepinephrine, 100 U/ml
233   penicillin, 100 µg/ml streptomycin and 2 mM L-glutamine (all reagents purchased from
234   Sigma-Aldrich, Italy) at 37°C in a humidified 5% CO2 incubator. The cells were seeded ($2x10^5$ cells
235   /ml) in 24-well culture plates containing a glass coverslip in each well coated with 25 µg/ml
236   fibronectin/0.02 % w/v gelatine solution (Sigma-Aldrich). The culture medium was changed every 3
237   days with fresh medium.

238   At 70-80% of confluence HL1 cells were exposed to 20-minutes of sound sequences. We used
239   this specific time period because we wanted to begin to study *in vitro* any possible direct effect of
240   sound that could help to explain the results that we are obtaining *in vivo* in other researches[51].

241   We choose atrial cardiomyocytes for their contractility, in order to try directly to visualize with
242   the Time-lapse technique (movies S-1 and S-2) possible changes of contraction in response to the
243   mechanical stress related to the sound waves used. After seeing a differential behavior with specific
244   sounds, we proceeded with the qualitative molecular analyzes, repeating the experiment 6 times,
245   always with the same results.

246   *Time-lapse images.* Cells at 80% confluence were analysed in live imaging using a Leica
247   DMI6000CS microscope (Leica Microsystems, Wetzlar, Germany) equipped with an incubator, with
248   a temperature-controller set at 37 °C and in a humified 5% CO2 atmosphere. The cells were acquired
249   every 100 or 160 msec for 20 min using a phase contrast (Ph) or a differential interference contrast
250   (DIC) at 20x/0.4 or 40x/0.6 objectives respectively. Images were acquired using a DFC365FX camera
251   and using the Leica Application Suite (LAS-AF) 3.1.1. software (Leica Microsystems). Some
252   time-lapse experiments were performed in the presence of 250 nM MitoTracker® Red (Thermo Fisher
253   Scientific, USA) probe for 20 min, a specific mitochondrial marker.

254   *Immunofluorescence and confocal microscopy.* Immediately after the treatment of the cells with the
255   different sounds, the cells were washed twice with phosphate buffered saline (PBS, 137 mmol/l
256   NaCl, 2.6 mmol/l KCl, 8 mmol/l Na_2HPO_4, 1.4 mmol/l KH_2PO_4, pH 7.4) and fixed in 2%
257   paraformaldehyde for 20 min, permeabilized with 0.5% Triton X-100 in PBS for 15 min and treated
258   with 0.05 mol/l NH_4Cl for 15 min. All steps were performed at room temperature. Subsequently,
259   cells were stained with the following antibodies; mouse anti-alpha-tubulin (α-tubulin) (EXBIO
260   Praha, Czech Republic) diluted 1:500, Alexa Fluor 488-Phalloidin diluted 1:150 to visualize F-actin
261   and rabbit anti-alpha-actinin-1 (Thermo Fisher Scientific, USA) diluted 1:25, all the antibodies were
262   incubated for 1h at 37°C. Rabbit anti-beta actin (β-actin) (Thermo Fisher Scientific, USA) diluted
263   1:200 was incubated over night at 4°C. The cells, after incubation with the primary antibodies, were
264   stained with the following specific secondary antibodies; 1:100-diluted fluorescein isothiocyanate
265   (FITC)-conjugated goat anti-mouse IgG (Chemicon International, Billerica, MA,USA), 1:200-diluted
266   Alexa Fluor 594-labelled goat anti-rabbit IgG (Life Technologies). The primary and secondary
267   antibodies were diluted in PBS containing 0.5% bovine serum albumin (BSA). Secondary antibodies
268   were also used in the absence of primary antibodies in order to assess non-specific binding. For the
269   immunofluorescence analysis, the cell nuclei were labelled with 1.5 µg/ml Hoechst 33258
270   (Sigma-Aldrich) for 20 min at room temperature. Finally, the slides were mounted with Mowiol
271   anti-fade solution (Sigma-Aldrich).

272   Leica DMI6000CS fluorescence microscope (Leica Microsystems) was used and samples were
273   analysed with differential interference contrast (DIC) and fluorescence objectives. Images were
274   acquired at 40x/0.60 dry objective magnification. Images were acquired using a DFC365FX camera
275   and using the Leica Application Suite (LAS-AF) 3.1.1. software.

276   The same samples were analysed by a confocal microscope TCS SP8 (Leica Microsystem) with a
277   z-interval of 1.5 µm using a 100x/1.4 oil immersion objective (image size 1024x1024 pixel). Images
278   were acquired with the above described camera and software.

279   Finally we measured the mean gray scale values (mean fluorescence intensity) of the markers
280   phalloidin, beta-actin and alpha-actinin-1 using three different Regions Of Interest (ROI) taken in
281   three different confocal images of the same marker, using the specific statistic function of the
282   LAS-AF 3.1.1. software (Leica Microsystems). Mean fluorescence intensity data were compared
283   using Mann-Whitney test for independent samples.

284

Supplementary Materials

Figure S1. Our laboratory set up for the experiment. A laptop computer with the audio tracks (A) is connected to an amplifier (B) positioned nearby the microscope (C) and its incubator (E). With a phonimeter we calibrated the volume of the amplifier so that the intensity of the sound in the point where the cells are positioned (E) is about 60 dB. which the intensity corresponds to a normal vocal conversation. (D1) CO2 controller, (D2) heating unit, temperature control unit (D3). We want to specify that also "control cells" were exposed to the speaker plugged to energy without any sound produced in order to exclude that our findings could be the result of any small vibration produced by the speaker itself instead of the sound. Finally, the sounds "Ti amo", "Ti odio" and the sound used in meditation were pronounced by 3 different people, giving the same results.
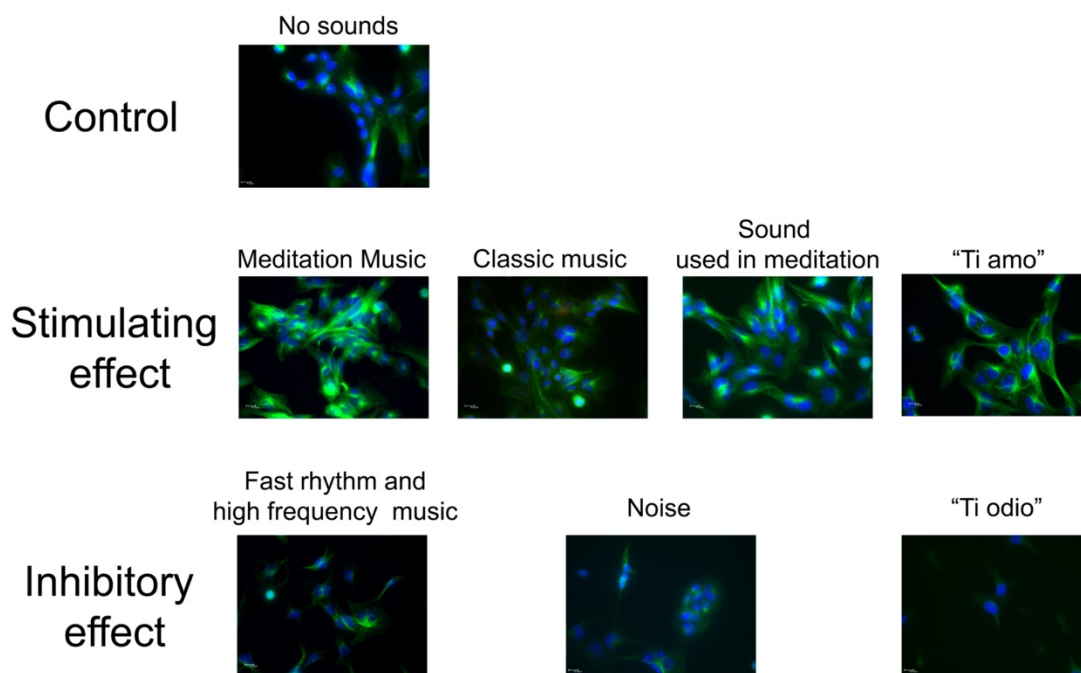
Figure S2. Alpha tubulin (α-tubulin) stained after treatment with different sounds for 20 min. The cells received the sound from right to left. HL1 cells were stained with α-tubulin (green fluorescence) and the nuclei were stained with Hoechst 33258 (blue fluorescence). The images show the merge of the two fluorescence at 63x/1.4 oil objective. In the first line, control cells without any sound treatment showing casual organization of cells and normal expression of the different markers. The middle line shows the stimulating/organizing effects of meditative and classic music, of a sound used in meditation and "Ti amo" sound. It is possible to observe the increased expression of α-tubulin. The third line depicts the inhibiting effects of high speed and high frequency music, noise (a collection of traffic noises and screams) and "Ti odio" sound. It is possible to observe the decreased expression of α-tubulin and the reduced number of cells. Scale bar 10μm.

Movie S1. Time-lapse video (images taken for 20 minutes every 160 msec) of HL-1 cardiomyocytes. A) controls, no sounds. B) "Ti amo" sound exposition. Please notice the increase in cell's motility and in the inner vesicular trafficking, compared with the control. C) Please notice cellular explosion during the "Ti odio" sound exposition. In some frames, the images may seem a bit fuzzy: it is a normal consequence of shooting in 2D, a 3D structure while moving.

Movie S2. Time-lapse video (images taken for 20 minutes every 100 msec) acquired on the same field. This video shows the behavior of the same HL-1 cardiomyocytes during 20 minutes of spontaneous growth/activity without any sounds (A) followed by the "Ti amo" (B) and the "Ti odio" (C) sound exposition. Please notice the increase in cell's contractility and the increased number of cells that start to beat in B. Finally, observe the decreased and asynchronous cell's contractility in C and the cessation of the beating of some cells. In some frames, the images may seem a bit fuzzy: it is a normal consequence of shooting in 2D, a 3D structure while moving.

Movie S3. The video shows the different geometric shapes of the wave trains linked to the words "Ti amo" and "Ti odio" while traveling in water. A drop of water was placed in a Petri dish placed above a vibro-acoustic plate (VIBBRO srl-Italy) connected to a computer. The audio files are emitted by the PC and the plate vibrates according to the specific frequencies of the sound, describing different geometric patterns both on the surface and on the thickness of the aqueous medium. This could mimic what occurs inside a cell and how all the molecules inside it oscillate. We did not use this platform during the experiment (please see fig.S1). This platform served only to show how a vibration can spread in a watery environment, similar to the cytoplasm.

326 **Movie S4**. Acoustics and vibration animations (courtesy of Dr. Daniel Russel, Pennsylvania State University):
327 the video shows how a particle placed in an aqueous environment (such as the cytoplasm) can move and
328 oscillate (in compression and rarefaction cycles) as a function of the longitudinal and transversal component of
329 the mechanical wave (sound) that passes it. We speculate that this movement could influence and regulate the
330 interactions between the intracytoplasmic molecules and cell to cell communication. The different frequencies
331 that make up a sound can travel compact in the case of a non-dissipative medium or separate into wave trains
332 with different speeds in the case of a dissipative medium (such as the cytoplasm). The proteins polymers can
333 undergo specific torsional deformations that could be influenced by mechanical waves such as sound waves.
334

References

1. Albrecht-Buehler G. Rudimentary form of cellular 'vision'. *Proc Natl Acad Sci U S A* 1992;**89**:8288 [PMID: 1518860 DOI: 10.1073/pnas.89.17.8288]

2. Albrecht-Buehler G. A long-range attraction between aggregating 3T3 cells mediated by near-infrared light scattering. *Proc Natl Acad Sci U S A* 2005;[PMID: 15790680 DOI: 10.1073/pnas.0407763102]

3. Sahu S, Ghosh S, Fujita D, Bandyopadhyay A. Live visualizations of single isolated tubulin protein self-assembly via tunneling current: effect of electromagnetic pumping during spontaneous growth of microtubule. *Sci Rep* 2014;**4**:7303 [PMID: 25466883 DOI: 10.1038/srep07303]

4. Sahu S, Ghosh S, Hirata K, Fujita D, Bandyopadhyay A. Multi-level memory-switching properties of a single brain microtubule. *Appl Phys Lett* 2013;[DOI: 10.1063/1.4793995]

5. Havelka D, Cifra M, Kučera O, Pokorný J, Vrba J. High-frequency electric field and radiation characteristics of cellular microtubule network. *J Theor Biol* 2011;**286**:31–40 [PMID: 21782830 DOI: 10.1016/j.jtbi.2011.07.007]

6. Pelling AE, Sehati S, Gralla EB, Valentine JS, Gimzewski JK. Local nanomechanical motion of the cell wall of Saccharomyces cerevisiae. *Science* 2004;**305**:1147–50 [PMID: 15326353 DOI: 10.1126/science.1097640]

7. Haase K, Pelling AE. Investigating cell mechanics with atomic force microscopy. *J R Soc Interface* 2015;**12**:20140970 [PMID: 25589563 DOI: 10.1098/rsif.2014.0970]

8. Gimzewski JK, Pelling AE, Ventura C. Nanomechanical characterization of cellular activity. 2008;International Publication Number WO 2008/105919 A3

9. Uzer G, Thompson WR, Sen B, Xie Z, Yen SS, Miller S, Bas G, Styner M, Rubin CT, Judex S, Burridge K, Rubin J. Cell Mechanosensitivity to Extremely Low-Magnitude Signals Is Enabled by a LINCed

373   Nucleus. *Stem Cells* 2015;**33**:2063–76 [DOI: 10.1002/stem.2004]

374   10.   Rubin C, Turner AS, Bain S, Mallinckrodt C, McLeod K. Low mechanical signals strengthen long bones.
375   *Nature* 2001, **412**:603–4 [PMID: 11493908 DOI: 10.1038/35088122]

376   11.   Rubin CT, Capilla E, Luu YK, Busa B, Crawford H, Nolan DJ, Mittal V, Rosen CJ, Pessin JE, Judex S.
377   Adipogenesis is inhibited by brief, daily exposure to high-frequency, extremely low-magnitude
378   mechanical signals. *Proc Natl Acad Sci U S A* 2007;**104**:17879–84 [PMID: 17959771 DOI:
379   10.1073/pnas.0708467104]

380   12.   Ozcivici E, Luu YK, Adler B, Qin Y-X, Rubin J, Judex S, Rubin CT. Mechanical signals as anabolic agents
381   in bone. *Nat Rev Rheumatol* 2010;**6**:50–9 [PMID: 20046206 DOI: 10.1038/nrrheum.2009.239]

382   13.   Facchin F, Bianconi E, Canaider S, Basoli V, Biava PM, Ventura C. Tissue Regeneration without Stem
383   Cell Transplantation: Self- Healing Potential from Ancestral Chemistry and Physical Energies. *Stem Cell*
384   *Int* 2018;**ID 7412035**:8 [DOI: 10.1155/2018/7412035]

385   14.   Martens EA, Thutupalli S, Fourrière A, Hallatschek O. Chimera states in mechanical oscillator
386   networks. *Proc Natl Acad Sci U S A* 2013;**110**:10563–7 [PMID: 23759743 DOI: 10.1073/pnas.1302880110]

387   15.   Matsuhashi M, Pankrushina AN, Takeuchi S, Ohshima H, Miyoi H, Endoh K, Murayama K, Watanabe
388   H, Endo S, Tobi M, Mano Y, Hyodo M, Kobayashi T, Kaneko T, Otani S, Yoshimura S, Harata A,
389   Sawada T. Production of sound waves by bacterial cells and the response of bacterial cells to sound. *J*
390   *Gen Appl Microbiol* 2005;**44**:49–55 [DOI: 10.2323/jgam.44.49]

391   16.   Babayi T, Riazi GH. The Effects of 528 Hz Sound Wave to Reduce Cell Death in Human Astrocyte
392   Primary Cell Culture Treated with Ethanol. *J Addict Res Ther* 2017;**08** [DOI: 10.4172/2155-6105.1000335]

393   17.   Lestard NR, Capella MAM. Exposure to Music Alters Cell Viability and Cell Motility of Human
394   Nonauditory Cells in Culture. *Evidence-based Complement Altern Med* 2016;[PMID: 27478480 DOI:
395   10.1155/2016/6849473]

396   18.   Lestard NDR, Valente RC, Lopes AG, Capella MAM. Direct effects of music in non-auditory cells in
397   culture. *Noise Health* 2013;**15**:307–14 [PMID: 23955127 DOI: 10.4103/1463-1741.116568]

398   19.   Lenzi P, Frenzili G, Gesi M, Ferrucci M, Lazzeri G, Fornai F, Nigro M. DNA damage associated with
399   ultrastructural alterations in rat myocardium after loud noise exposure. *Environ Health Perspect*
400   2003;**111**:467–71 [DOI: 10.1289/ehp.5847]

401   20.   Antunes E, Borrecho G, Oliveira P, de Matos APA, Brito J, Águas A, Martins dos Santos J. Effects of
402   low-frequency noise on cardiac collagen and cardiomyocyte ultrastructure: An immunohistochemical
403   and electron microscopy study. *Int J Clin Exp Pathol* 2013;**6**:2333–41

404   21.   Uchiyama M, Jin X, Zhang Q, Hirai T, Amano A, Bashuda H, Niimi M. Auditory stimulation of opera
405   music induced prolongation of murine cardiac allograft survival and maintained generation of
406   regulatory CD4+CD25+ cells. J. Cardiothorac. Surg.2012;**7**:26 [PMID: 22445281 DOI:
407   10.1186/1749-8090-7-26]

408   22.   Ventura C, Graves M, Bergonzoni A, Tassinari R, Cavallini C. Cell melodies : when sound speaks to
409   stem cells. *CellR4* 2017;**5**:e2331

410   23.   Naseer SM, Manbachi A, Samandari M, Walch P, Gao Y, Zhang YS, Davoudi F, Wang W, Abrinia K,
411   Cooper JM, Khademhosseini A, Shin SR. Surface acoustic waves induced micropatterning of cells in
412   gelatin methacryloyl (GelMA) hydrogels. *Biofabrication* 2017;**9**:015020 [PMID: 28195834 DOI:
413   10.1088/1758-5090/aa585e]

414   24.   Guo F, Li P, French JB, Mao Z, Zhao H, Li S, Nama N, Fick JR, Benkovic SJ, Huang TJ. Controlling cell–
415   cell interactions using surface acoustic waves. *Proc Natl Acad Sci* 2015;**112**:43–8 [PMID: 25535339 DOI:
416   10.1073/pnas.1422068112]

417   25.   Havelka D, Kučera O, Deriu MA, Cifra M. Electro-acoustic behavior of the mitotic spindle: a
418   semi-classical coarse-grained model. *PLoS One* 2014;**9**:e86501 [PMID: 24497952 DOI:
419   10.1371/journal.pone.0086501]

420   26.   Kučera O, Havelka D, Cifra M. Vibrations of microtubules: Physics that has not met biology yet. *Wave
421   Motion* 2017;**72**:13–22 [DOI: 10.1016/j.wavemoti.2016.12.006]

422   27.   Wang N, Tytell JD, Ingber DE. Mechanotransduction at a distance: Mechanically coupling the
423   extracellular matrix with the nucleus. *Nat. Rev. Mol. Cell Biol.* 2009;**10**:75–82 [PMID: 19197334 DOI:
424   10.1038/nrm2594]

425   28.   Guzun R, Karu-Varikmaa M, Gonzalez-Granillo M, Kuznetsov A V., Michel L, Cottet-Rousselle C,
426   Saaremäe M, Kaambre T, Metsis M, Grimm M, Auffray C, Saks V. Mitochondria-cytoskeleton
427   interaction: Distribution of β-tubulins in cardiomyocytes and HL-1 cells. *Biochim Biophys Acta - Bioenerg*
428   2011;**1807**:458–69 [DOI: 10.1016/j.bbabio.2011.01.010]

429   29.   Kuznetsov A V., Javadov S, Guzun R, Grimm M, Saks V. Cytoskeleton and regulation of mitochondrial
430   function: The role of beta-tubulin II. *Front Physiol* 2013;**4 APR** [DOI: 10.3389/fphys.2013.00082]

431   30.   Chang CT, Bostwick JB, Steen PH, Daniel S. Substrate constraint modifies the Rayleigh spectrum of
432   vibrating sessile drops. *Phys Rev E - Stat Nonlinear, Soft Matter Phys* 2013;**88**:23015 [DOI:
433   10.1103/PhysRevE.88.023015]

434   31.   Kučera O, Havelka D. Mechano-electrical vibrations of microtubules-Link to subcellular morphology.
435   *BioSystems* 2012;**109**:346–55 [DOI: 10.1016/j.biosystems.2012.04.009]

436   32.   Misawa T, Takahama M, Kozaki T, Lee H, Zou J, Saitoh T, Akira S. Microtubule-driven spatial
437   arrangement of mitochondria promotes activation of the NLRP3 inflammasome. *Nat Immunol*
438   2013;**14**:454–60 [PMID: 23502856 DOI: 10.1038/ni.2550]

439   33.   Peleg B, Disanza A, Scita G, Gov N. Propagating cell-membrane waves driven by curved activators of
440   actin polymerization. *PLoS One* 2011;**6**:1–11 [DOI: 10.1371/journal.pone.0018635]

441   34.   Dierkes K, Sumi A, Solon J, Salbreux G. Spontaneous Oscillations of Elastic Contractile Materials with
442   Turnover. *Phys Rev Lett* [Internet] 2014 [cited 2019 Apr 2];**113**:148102 [DOI:

443   10.1103/PhysRevLett.113.148102]

444 35. Bányai LA. A Compendium of Solid State Theory. *Springer International Publishing;* 2018.

445 36. Maldovan M. Sound and heat revolutions in phononics. *Nature* 2013;**503** [DOI: 10.1038/nature12608]

446 37. Meijer DKF, Geesink HJH. Guided Folding of Life's Proteins in Integrate Cells with Holographic
447   Memory and GM-Biophysical Steering. *Open J Biophys* 2018;**08**:117–54 [DOI: 10.4236/ojbiphy.2018.83010]

448 38. Meijer DKF, Geesink JH. Phonon Guided Biology. Architecture of Life and Conscious Perception Are
449   Mediated by Toroidal Coupling of Phonon, Photon and Electron Information Fluxes at Discrete
450   Eigenfrequencies. *NeuroQuantology* 2016;**14** [DOI: 10.14704/nq.2016.14.4.985]

451 39. Acbas G, Niessen KA, Snell EH, Markelz AG. Optical measurements of long-range protein vibrations.
452   *Nat Commun* 2014;**5**:3076 [DOI: 10.1038/ncomms4076]

453 40. Gerlich S, Eibenberger S, Tomandl M, Nimmrichter S, Hornberger K, Fagan PJ, Tüxen J, Mayor M,
454   Arndt M. Quantum interference of large organic molecules. *Nat Commun* 2011;**2**:263 [PMID: 21468015
455   DOI: 10.1038/ncomms1263]

456 41. Zhang S, Cheng J, Qin YX. Mechanobiological modulation of cytoskeleton and calcium influx in
457   osteoblastic cells by short-term focused acoustic radiation force. *PLoS One* 2012;**7**:e38343 [DOI:
458   10.1371/journal.pone.0038343]

459 42. Kamkin A, Kiseleva I. Mechanosensitivity and Mechanotransduction. *Springer Netherlands*; 2011.

460 43. Mavromatos NE. Non-linear dynamics in biological microtubules: Solitons and dissipation-free energy
461   transfer. In: Journal of Physics: Conference Series. IOP Publishing; 2017.

462 44. Mańka R, Ogrodnik B. A model of soliton transport along microtubules. *J Biol Phys* 1991;**18**:185–9 [DOI:
463   10.1007/BF00417807]

464 45. Abdalla E, Maroufi B, Melgar BC, Sedra MB. Information transport by sine-Gordon solitons in
465   microtubules. *Phys A Stat Mech its Appl* 2001;**301**:169–73 [DOI: 10.1016/S0378-4371(01)00399-5]

466 46. Liu D, Every AG, Tománek D. Long-wavelength deformations and vibrational modes in empty and
467   liquid-filled microtubules and nanotubes: A theoretical study. *Phys Rev B* 2017;**95**:205407 [DOI:
468   10.1103/PhysRevB.95.205407]

469 47. Prodan E, Prodan C. Topological Phonon Modes and Their Role in Dynamic Instability of Microtubules.
470   *Phys Rev Lett* 2009;**103**:248101 [DOI: 10.1103/PhysRevLett.103.248101]

471 48. Prodan E, Dobiszewski K, Kanwal A, Palmieri J, Prodan C. Dynamical Majorana edge modes in a broad
472   class of topological mechanical systems. *Nat Commun* 2017;**8**:14587 [DOI: 10.1038/ncomms14587]

473 49. Aghaei A, Dayal K, Elliott RS. Symmetry-adapted phonon analysis of nanotubes. *J Mech Phys Solids*
474   2013;**61**:557–78 [DOI: 10.1016/j.jmps.2012.09.008]

475   50.   Zandonella C. Dying cells dragged screaming under the microscope. *Nature* 2003;**423**:106–7 [DOI:
476   10.1038/423106b]

477   51.   Dal Lin C, Marinova M, Rubino G, Gola E, Brocca A, Pantano G, Brugnolo L, Sarais C, Cucchini U,
478   Volpe B, Cavalli C, Bellio M, Fiorello E, Scali S, Plebani M, Iliceto S, Tona F. Thoughts modulate the
479   expression of inflammatory genes and may improve the coronary blood flow in patients after a
480   myocardial infarction. *J Tradit Complement Med* 2018;**8**:150–63 [PMID: 29322004 DOI:
481   10.1016/j.jtcme.2017.04.011]

482   Appendix 1 - *In vitro* effects on cellular shaping, contratility, cytoskeletal organization and
483   mitochondrial activity in HL1 cells after different sounds stimulation. A qualitative
484   pilot study and a theoretical physical model.

The theoretical physical model

486   In this Appendix we discuss the effects on cells and their components that are induced by different sounds,
487   pressure waves and mechanical vibrations, which we will refer to generically as 'sounds'. We will resort to
488   results reported in Refs.[1,2,3]. We call 'positive' sounds those producing ordering, formation of protein
489   'bridges', cell-to-cell correlations, strengthening of the links in the cytoskeleton network, etc., resulting in an
490   augmented biological activity. The 'negative' sounds induce instead negative response, i.e. the inhibition of the
491   ordering among biological components, sometimes presenting even the cell destruction (cell 'explosion')) (see
492   Figs. 1-3, S2, Movies S1 and S2. See Figs. A1, A2, A3 for the representations of three sound signals).

493   A characteristic feature of quantum field theory (QFT) is the distinction between the symmetry properties
494   of the states of the system and those of the dynamical equations. When the symmetry properties of the system
495   ground state are not the same ones of the dynamical equations, we have the phenomenon of spontaneous
496   breakdown of symmetry (SBS) which manifests itself in the generation of ordering ('spontaneous' means that
497   the system dynamics selects self-consistently the system ordering). The formation of ordered patterns is due to
498   long range correlations among the system constituents. The quanta associated to such long range waves, called
499   the Nambu-Goldstone (NG) boson quanta, condense in the system ground state [4,5,6].

501   In biological matter, macromolecules are characterized by the specific electric dipole moment of their
502   constituent units. Macromolecules and cells are embedded in the water bath. Water molecules, which
503   constitute the large majority in number of the present molecules are also characterized by their specific electric
504   dipole moment. Since dipoles may be oriented in any direction, the basic symmetry is the rotational spherical
505   symmetry. The action of some external input, e.g. sounds, may trigger the breakdown of the dipole rotational
506   symmetry by producing dipole ordering, namely their alignment along a preferred direction, or their in phase
507   oscillations. The state of the system will be then characterized by the non-vanishing polarization density *P(x,t)*
508   which provides a measure of the ordering (the electret) and it is therefore called "order parameter". The NG
509   quanta of the long range correlations responsible of the ordering are called dipole wave quanta (dwq) [1,2]. The
510   generation of the dipole long range correlations facilitates the occurrence of short range interactions, such as
511   Van der Waals interactions, H-bonding, etc. by reducing the randomness of the molecular kinematics so to
512   enhance the observed high efficiency of metabolic reactions. Long range correlations allow the collective,
513   *coherent* behavior of the system components which manifests itself in the macroscopic scale behavior of the
514   observed cellular structures and cell network.

515

516   Beside the sound induced SBS in the cell environment and in the water bath where the cells are embedded,

517   there is another remarkable effect produced by sounds on quasi-unidimensional structures, such as protein

518   chains. The energy supplied by the sounds hitting the extremity of a protein molecular chain may produce

519   indeed a deformation in the chain turning into oscillations of the electric dipoles of the chain units. The

520   conformational change, coupled to the chain molecular dipoles, traveling over the chain as a localized

521   deformation is ruled by the nonlinear Schrödinger equation. It is known as the Davydov soliton, or Davydov

522   solitary wave, so called since it remains stable under collision with other similar waves [7,8,9].

523

524   The energy necessary to excite the Davydov soliton is of the order of *0.25* eV, which is the energy released

525   by ATP hydrolysis at the origin of a protein chain [1,2,3,7]. In addition to the possibility that the sound directly

526   couples to the chain, we may also suppose that the energy supplied by the sound triggers the ATP reaction and

527   this one in turn triggers the soliton formation on the protein. It is not relevant to our analysis which one of these

528   possibilities is actually realized. In both possible cases, the response of the protein chain to the sound is the

529   propagation in the form of the Davydov solitary wave of the *coherent* localized deformation, i.e. of *in phase*

530   dipole vibrational modes. In many-body physics the 'coherent dynamics' is indeed the one ruling the "in phase

531   motion" of a collection of elementary components [1,2,3,4,5,6].

532

533   We list few of the properties of the dynamical scenario implied by the soliton:

534   i) The solitary wave has a 'nondissipative' propagation. This means that contrarily to the usual (non-solitary)

535   wave motion, the soliton does not lose (or loses very little amount of) its energy during its traveling on the

536   protein chain and can propagate over large distances. Since the discreteness of the chain may produce periodic

537   potentials, the soliton velocity may be a function of time [8].   The energy supplied by the sound to the system

538   may remain thus 'trapped' in the solitary wave and it is then transferred along the protein chain (almost) without

539   dissipation. In the absence of such a dynamical mechanism an excess of sound energy supplied to the cell, with

540   a frequency spectrum unable to resonate with the molecular oscillatory motion of the cell constituents, might

541   lead to the excessive warming up of the cell, possibly leading to its explosion, as observed in the case of

542   'negative' sounds.

543   ii) The oscillations of the chain molecular dipoles propagating with the soliton produce an electromagnetic

544   (e.m.) radiation. Such a radiation constitute an endogenous source of e.m. field and will then break the rotational

545   symmetry of the surrounding water molecular dipoles with their consequent coherent oscillation and

546   orientation. Spectroscopic observations under ambient conditions have indeed shown [10] that hydration water

547   forms a superstructure of the macromolecule (DNA, in the experiment of Ref. [10]) with a strict interdependence

548   between deformations of the macromolecule chain and its water environment.

549

550   iii) A soliton is able to trap an electric charge in its motion (electrosoliton) [7,8,9]. This may then result in a

551   nondissipative electric current flowing (with the soliton) over the protein chain. The radiation emitted according

552   to the Maxwell equations, together with the one emitted by the chain dipole oscillations (point ii)), synchronizes

553   with the radiation emitted by solitons on the other proteins; they might then travel with the same velocity and

554   emit radiation at the same   frequency [9].

555

556   iv) The soliton traveling over an infinitely long chain is stable (infinite life-time). Protein chains have, however,

557   finite length. The Davydov soliton has then a finite life-time. It decays once in its propagation has reached the

558 end of the chain and will then release its trapped energy in the surrounding water bath. Such an energy will not

559 produce an increase of the bath temperature since the energy will propagate in it not in a diffusive way, but in

560 wave form because the bath has been brought in the electret (ordered) state by the same soliton (point ii)) before

561 its decay.

562

563   The supply of energy to the cell by the sound can be regarded as a "feeding" process of the cell. As

564 described above, such a feeding process triggers the spontaneous breakdown of the rotational symmetry of

565 surrounding water dipoles with the generation of the water electret state. The short life-time of the water electret

566 state suggests to us the cyclic process picture, by which, in order that the functional biological activity related to

567 the ordered cell state may continue, the cell needs to be fed again by an external resonating agent when the

568 electret state vanishes, and so on, in a cycle, indeed.

569   Summing up, the emerging picture seems to fit with the experimental observations reported in text for the

570 cases of 'positive' and 'negative' sounds. The 'negative' effects on the biological matter may be attributed to

571 the lack of the dynamic processes described above (cf. Figs. 1-3, S2, Movies S1 and S2).

572   The sound induced ordering processes considered above generate in turn another remarkable effect. It is

573 known that the e.m. field propagates in a self-focusing fashion through an ordered medium and acquires a finite

574 mass in its propagation (the Anderson-Higgs-Kibble (AHK) mechanism) [5,6]. This provides the understanding

575 of many phenomena in condensed matter physics and elementary particle physics. In our case, the mass M

576 acquired by the e.m. field turns out to be a function of the water polarization density $P(x,t)$, $M = M(P)$, $M(P) = 0$

577 at $P=0$, and the propagation of the field occurs in a filamentary-like fashion, as through channels piercing the

578 ordered medium (self-focusing) [11,12,13]. The Maxwell propagation in spherical waves is restored at $P(x,t) = 0$.

579 The relation between the radius d of the channel and M is $d = \hbar/cM$, for $M \neq 0, P \neq 0$, where $\hbar = h/2\pi$; h is

580 the Planck constant and c the speed of light.

581   The e.m. field propagation is thus confined within such channels in the polarized medium. Outside them its

582 intensity is zero. The transverse field gradient on the channel boundary acts on the atoms or molecular

583 aggregates in the region surrounding the channels as a selective force given by [2,14]

$$F = const\ \nabla E^2 \sum_k \frac{v_{0k}^2 - v^2}{(v_{0k}^2 - v^2)^2 + \Gamma_k^2} \ ,$$

585 where E is the electric field, v its frequency, Γ_k the damping of the molecular oscillations of frequency v_{0k}.

586 We see that the force is relevant for high field gradient and if the resonant condition $v_{0k} \simeq v$ is met. Moreover,

587 the force F is repulsive or attractive depending on the $\pm$ sign of the difference $(v_{0k}^2 - v^2)$, respectively,

588 which also shows that small changes in the frequencies near the resonant values, by producing switching

589 between the $\pm$ signs, induce switching between repulsive and attractive forces, respectively. Furthermore, the

590 field frequency within the channel may be perturbed by the presence of the molecule(s) previously attracted on

591 the channel boundary, thus making the force to be attractive (or repulsive) with respect to a molecule with

592 different v_{0k} . The result is that different molecules are selectively collected on the channel boundary. If such

593 molecules may form stable chemical bounds, a dynamical polymerization process is obtained and the polymeric

594 structure coating the channel survives also in the case that the e.m. field vanishes. In the opposite case of low

595 chemical affinity among the collected molecules, the molecular coating will disassemble with the vanishing of

596 the e.m. field. The molecular coating of the field channels may thus represent the observed process of dynamical

597 formation of network branches in the cell cytoskeleton and in cell to cell correlations, affecting their mobility

598 and contractility (cf. the text and Figs. 1,3, column V; S2, Movies S1 and S2).   In the case of a fraction α of

599 oriented water molecular dipoles, it can be shown [2,3] that $M = 13,60/\sqrt{\alpha}$ eV and $d = 146/\sqrt{\alpha}$ Å, to be compared

600   with *125* Å, the observed average radius of the cytoplasm microtubules. This suggests that $\alpha \simeq 1,4$, i.e. that
601   almost all the dipoles are correlated. Note that $E = 13,60$ eV is the hydrogen ionization energy, which may be
602   considered as a threshold energy. A photon of energy $h\nu > 13,60$ eV may propagate with a destructive effect
603   in the coherent dipole ordered region (with possible hydrogen ionization events), thus restoring the spherical
604   symmetry with loss of the filamentary e.m. propagation. On the other hand, a photon of lower energy may be
605   not able to penetrate the ordered patterns. Small amounts of supplied energy may contribute instead to the
606   increase of the polarization, being thus 'stored' within the system till a convenient accumulated amount may be
607   used for metabolic activity (e.g. the energy required for a specific chemical reaction to occur), or the threshold
608   *13,60* eV will be reached and then radiated in ionization processes or to open a channel through which
609   propagate (delayed propagation and radiation) [2,3,15]. The possibility of 'non-thermalizing' energy storage is
610   thus offered by coherence. In Fig. 1, the panel B-II shows that in the presence of the (positive) energy supply
611   stored in the environment, mitochondrial activity (finalized to supply energy) is resting with respect to the
612   activity shown in panel A-II (absence of sounds; control system).

614   The mass acquired by the e.m. field produces also a longitudinal component (beside the transvers one) [3].
615   This component acts as a force directed along the channel pushing the collected molecules, thus, depending on
616   their chemical affinity, either promoting their chemical interaction, or, producing disruption of the microtubule
617   (especially in its ending part, similarly to what observed in the microtubule treadmilling). On the other hand, it
618   is observed that most of the metabolic reactions occurs on the microtubule structures, which also acts as a sort of
619   transport rail system of the cell. We then may conclude that the transverse (attractive or repulsive) force may
620   produce the sequential ordering of interlocked chemical reactions on the microtubule, while its longitudinal
621   component contributes to the chemical transport cell system.

623   The processes described above crucially depend on the time dependent polarization density *P(x,t)*
624   produced in the cell and in the inter-cellular bath under the action of the external stimuli. Too much high
625   polarization density and its persistence for a too long time interval may prevent the e.m. field disturbance to
626   penetrate through the ordered medium in the described filamentary fashion and the subsequent described
627   processes will not occur. On the contrary, too much low *P(x,t)* and its too short life-time might allow to an even
628   low energy stimulus to fully destroy any polarization pattern. We thus see that the cell functional activity may
629   occur within a window limited by high and low values of the ordering produced by external stimuli.
630   Thermal effects are among the perturbing agents of the working conditions. Ordered patterns are described
631   in many-body physics in terms of condensation in the ground state of the NG quanta of the long range
632   correlation waves (the dwq in the present case), as mentioned above. In the approximation that the condensed
633   quanta behave as free particles in such a ground state, we have [2]:

634 $$\frac{p^2}{2m_{eff}} = \frac{3}{2} k_B T \ ,$$

635   where *T* is the temperature, *p* the momentum, k_B the Boltzmann constant and m_{eff} the effective mass of the
636   dwq due to the finite linear size $R = \hbar /cm_{eff}$ of the coherent domain. Use of the de Broglie relation $p = h/\lambda$, in
637   the stationary condition $R = n\,\lambda/2$, with *n* an integer, gives

638 $$R = \frac{\pi h c}{6 k_B} n^2 \frac{1}{T} \ .$$

639   At *T= 300* K, for *n = 1*, *R = 25* micron, which agrees with the order of magnitude of the observed structures (see
640   the scale reported in the Figures in the text). The above relation shows that in order to keep *T* constant, the

641 system reacts (opposes) to, e.g., an increase of T, due for example to an external supply of energy, by increasing

642 the linear size R of the coherent correlated region, i.e. shifting toward longer wave lengths correlations (for

643 fixed n). Similarly, it opposes   to a decrease of T by lowering the linear size R of the correlated region. We have

644 a dynamical reaction of the system aimed to preserve its functionality against thermal effects.

645

646 On the other hand, by considering the system in a given ordered state, i.e. with a given density N of

647 condensed dwq at a stationary temperature ((almost) constant T), the minimization of the free energy F

648 characterizes the system stationary state: $dF = dU - k_B T\, dS = 0$, with U the internal energy and S the entropy.

649 We then obtain [16,17]: $dU \propto dN/dt \propto k_B T dS$, where as usual we may define heat as $dQ = k_B T\, dS$, and

650 which shows that a supply of energy so to have $dU > 0$, implies $dS > 0$ and an increase of the rate of change of

651 dN/dt, i.e. an *increase in the loss* of condensed dwq, i.e. of correlations in the ground state, since $dS > 0$

652 implies loss of ordering. Thus we see the 'disordering effect' of the 'negative' sound releasing energy to the

653 system ($dU > 0$) in a 'non-resonant' way, possibly leading to the cell explosion. On the contrary, 'positive'

654 sounds producing ordering imply $dS < 0$, i.e. $dU < 0$ and $dN/dt < 0$, i.e. a *reduction of the loss* of correlations.

655 We also see the positive effect of dissipating energy by the system ($dU < 0$), provided that a critical threshold is

656 respected.

657

658 Another dynamical defense of the system against thermalization is due to the dynamical nonlinearity. The

659 system is made by a large number N of components. Their coupling to phonon and to e.m. field gets enhanced

660 by a factor $\sqrt{N}$ [18]. In the limit of large N, the collective interaction time scale is then shorter by a factor $1/\sqrt{N}$

661 than the short range interaction time scale among the individual components. The collective interaction is thus

662 protected against thermal fluctuations. These may interfere with the coherent dynamics only provided that $k_B T$

663 is comparable or larger than the collective interaction energy. This guaranties the character of collective

664 dynamics for the system as a whole, a result out of reach in a purely atomistic view and approach.

665

666 Finally, we mention that there is an isomorphism between coherent states and self-similarity fractal

667 properties [19,20] so that we expect that a possible difference between 'positive' and 'negative' signals may

668 consist in their self-similar fractal properties, either in their different fractal dimension,   or in having or not

669 having fractal structure, the 'positive' and the 'negative' ones, respectively, so that they can induce or not,

670 correspondingly, coherent state configurations with similar fractal properties in the biological matter. A

671 suggestion in such a direction comes to us from the plot in Fig. A3, which represents the signal of the sound

672 used in meditation (one of   the   "positive" sounds,   cf. its effects in Fig. S2). The linear fitting of the log of

673 power (on the ordinate axis) *vs* the log of frequency (on the absciss axis) shows the self-similarity structure of

674 the signal with fractal dimension $d = -2,14787E7$ (the slope of the fitting straight line). It is in our future plan

675 to analyze the fractal properties, if any, of the other used signals.

676

677 In conclusion, the QFT model seems to account for the observed effects that are produced by the diverse

678 sounds on the biological matter. Sounds may perturb the biological functional activity by enhancing or

679 inhibiting in the way described above the coherent dipole dynamics, the formation and propagation of solitons

680 and electrosolitons and the associated nondissipative transport on protein chains of energy and charges trapped

681 by them, the self-focusing propagation of the e.m. field, the formation and depletion of microtubules and of

682 links in the inter-cellular network.

683

References for appendix 1.

1. Del Giudice E, Doglia S, Milani M, Vitiello G. A quantum field theoretical approach to the collective behavior of biological systems. *Nucl Phys B* 1985; **251**(FS 13): 375 – 400.

2. Del Giudice E, Doglia S, Milani M, Vitiello G. Electromagnetic field and spontaneous symmetry breakdown in biological matter. *Nucl. Phys. B* 1986; **275**(FS 17):185 – 199.

3. Del Giudice E, Doglia S, Milani M, Vitiello G. Structure, correlations and electromagnetic interactions in living matter: Theory and applications. In *Biological coherence and response to external stimuli*, H. Fröhlich Ed., Springer-Verlag, Berlin, 1988; 49 – 64.

4. Goldstone J, Salam, A, Weinberg, S. Broken Symmetries, *Phys. Rev* 1962; **127**: 965 – 970.

5. Umezawa H. *Advanced field theory: Micro, macro, and thermal physics*. New York, AIP, 1993.

6. Blasone M, Jizba P, Vitiello G. *Quantum Field Theory and its macroscopic Manifestations*, Imperial College Press, London, 2011.

7. Davydov A S. *Solitons in Molecular System*. Dordrecht, Reidel,1985.

8. Brizhik L, Cruzeiro-Hansson L, Eremko A, Olkhovska Yu. Soliton dynamics and Peierls-Nabarro barrier in a discrete molecular chain. *Phys Rev B* 2000; **61**(2): 1129 – 1141.

9. Brizhik L. Influence of electromagnetic field on soliton mediated charge transport in biological systems. *Electromagn Biol Med* 2015;**34**(2): 123 –132 (ID: 1036071; DOI:10.3109/15368378.2015.1036071).

10. McDermott M L, Vanselous H, Corcelli S A, PetersenP B. DNA's Chiral Spine of Hydration. *ACS Cent Sci* 2017; **3** (7) : 708 – 714.

11. Marburgher J H. Self-focusing. *Theory Prog Quant Electr* 1975; **4**:35 – 110.

12. Chiao R Y, Gustafson T K and Kelley P L. Self-Focusing of Optical Beams. In: Boyd, R. W., Lukishova, S G. and Shen, Y R. (Eds.), *Self Focusing: Past and Present*. Springer, New York, 2009; 129 -143.

13. Zakharov V E, Shabat A B. Exact theory of two-dimensional self-focusing and automodulation of waves in nonlinear media. *Sov J Exp Theor Phys* 1971; **61**:118–134.

14. Askar'yan G A. The self-focusing effect. *Sov phys Usp 1974 ;***16**: 680.

15. Mandoli D F, Briggs W. Optical properties of etiolated plant tissues. *Proc Nat Acad Sc USA* 1982; **79**: 2902 – 2906.

16. Celeghini E, Rasetti M, Vitiello G. Quantum dissipation. *Annals of Physics (N.Y.)* 1992; **215**:156 – 170.

17. Vitiello G. Dissipation and memory capacity in the quantum brain model. *Int J Mod Phys* 1995; **B9**: 973 – 989.

18. Del Giudice E, Vitiello G. The role of the electromagnetic field in the formation of domains in the process of symmetry breaking phase transitions. *Phys Rev A* 2006; **74**: 02210, 5.

19. Vitiello G. Fractals, coherent states and self-similarity induced noncommutative geometry. *Phys. Lett. A* 2012; **376**: 2527– 2532 .

20. Vitiello G. Coherent states, fractals and brain waves. *New Mathematics and Natural Computing* 2009; **5**: 245– 264.
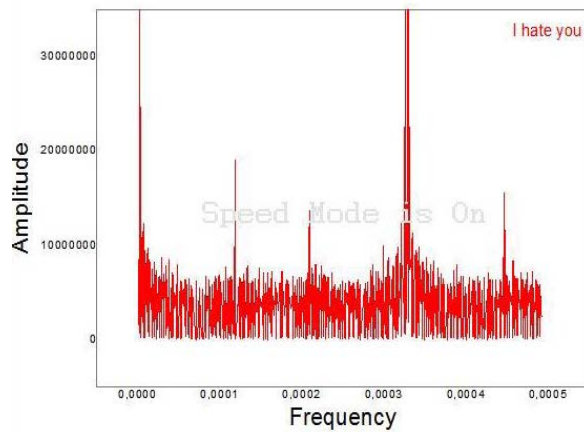
Fig. A1. Negative sound ("Ti odio"-I hate you) . Signal FFT (finite Fourier transform).
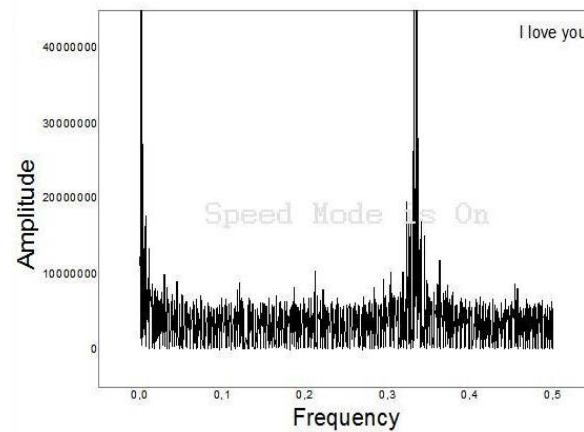

Fig. A2.   Positive sound ("Ti amo"- I love you). Signal FFT (finite Fourier transform).
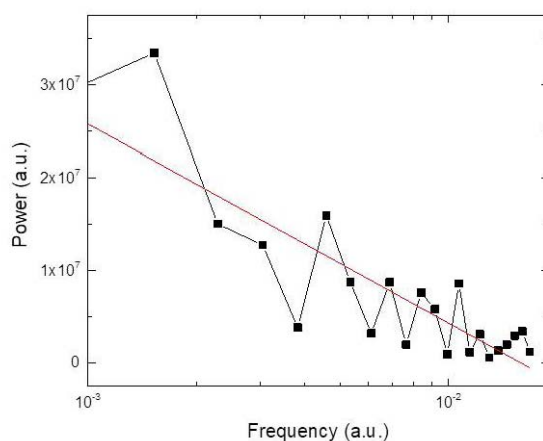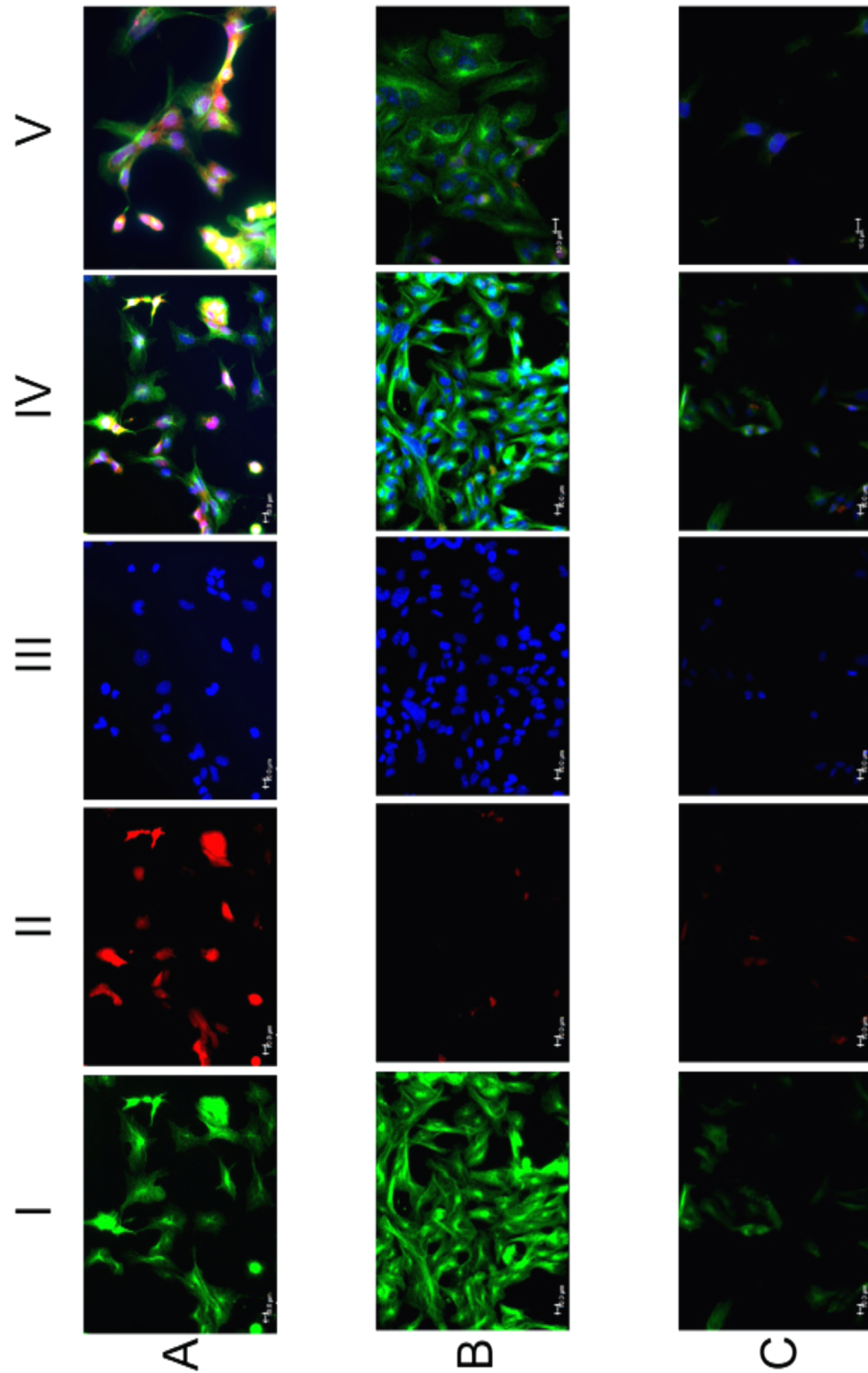

Fig.A3. Positive sound (Sound used in meditation). Log-log plot (Power *vs* frequency, arbitrary units).

Fractal dimension (straight line slope) d = -2,14787E7 (signal analyzed by use of Origin data analysis software).

Manuscript - Figure 1

C. Dal Lin and CM Radu et al." In vitro effects on cellular shaping, contratility, cytoskeletal organization and mitochondrial activity in HL1 cells after different sounds stimulation. A qualitative pilot study and a theoretical physical model". Figures.
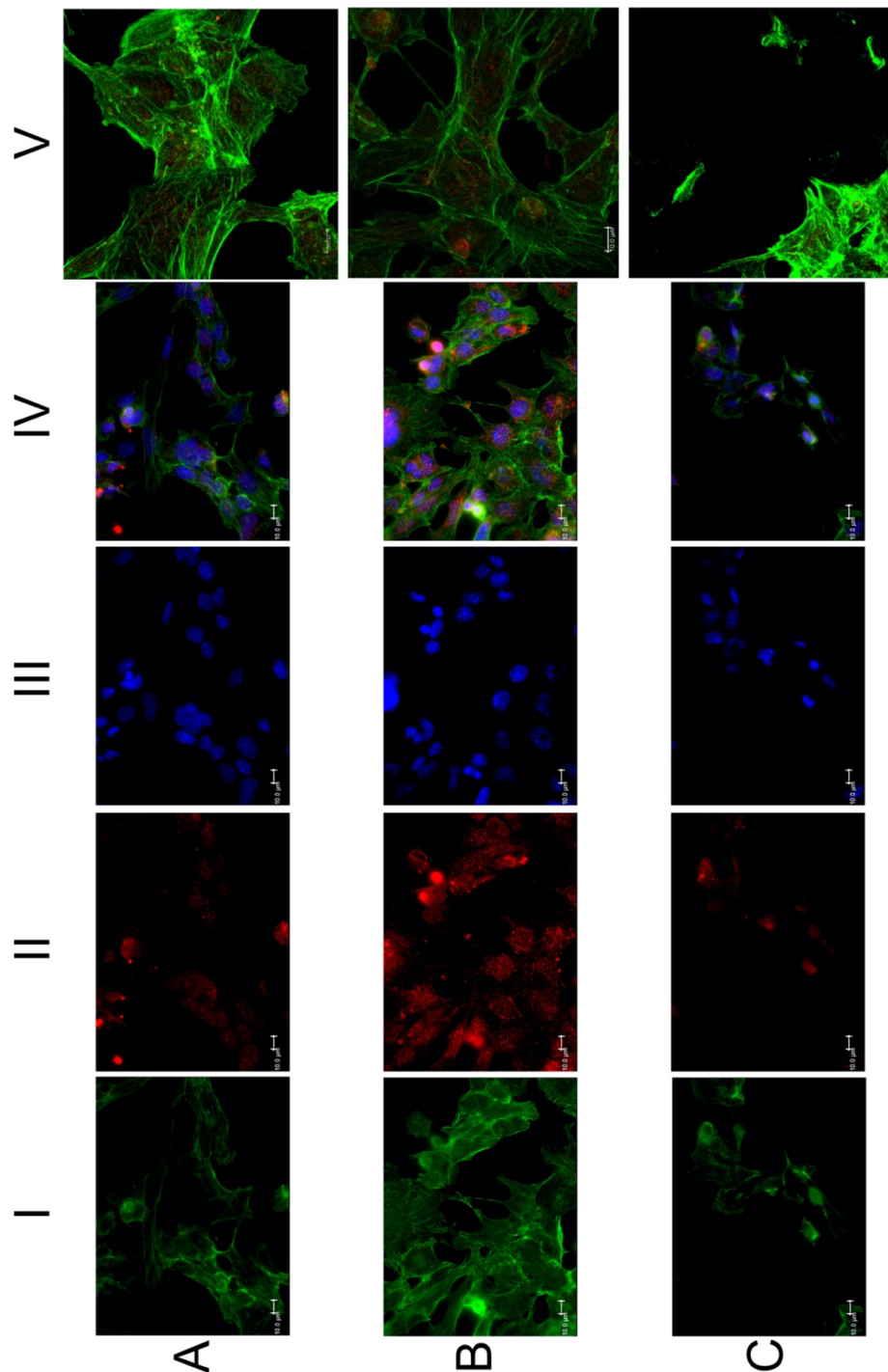
Manuscript – Figure 2

C. Dal Lin and CM Radu et al." In vitro effects on cellular shaping, contratility, cytoskeletal organization and mitochondrial activity in HL1 cells after different sounds stimulation. A qualitative pilot study and a theoretical physical model". Figures.
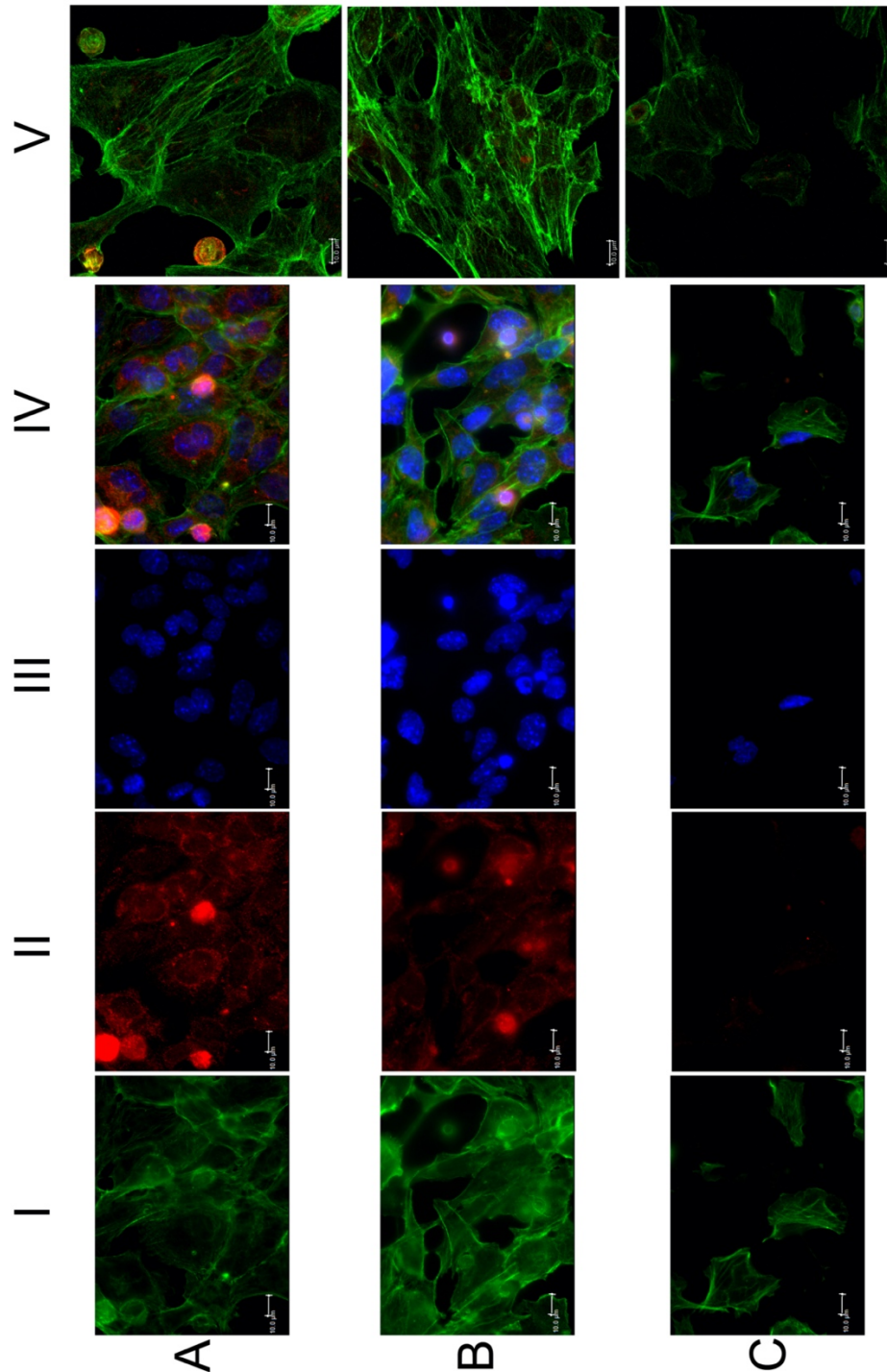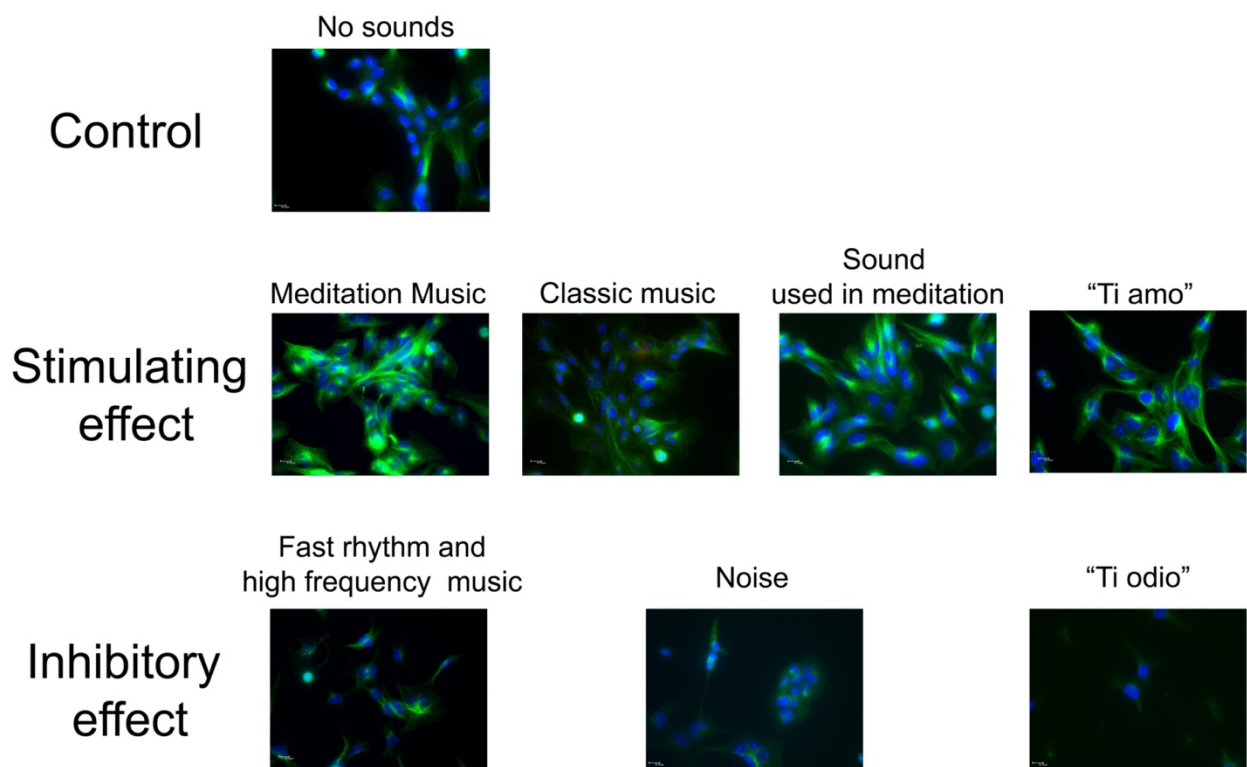
Manuscript – Figure 3

C. Dal Lin and CM Radu et al." *In vitro* effects on cellular shaping, contratility, cytoskeletal organization and mitochondrial activity in HL1 cells after different sounds stimulation. A qualitative pilot study and a theoretical physical model". Figures.

Supplements Figure S1

Supplements Figure S2

C. Dal Lin and CM Radu et al." *In vitro* effects on cellular shaping, contratility, cytoskeletal organization and mitochondrial activity in HL1 cells after different sounds stimulation. A qualitative pilot study and a theoretical physical model". Figures.
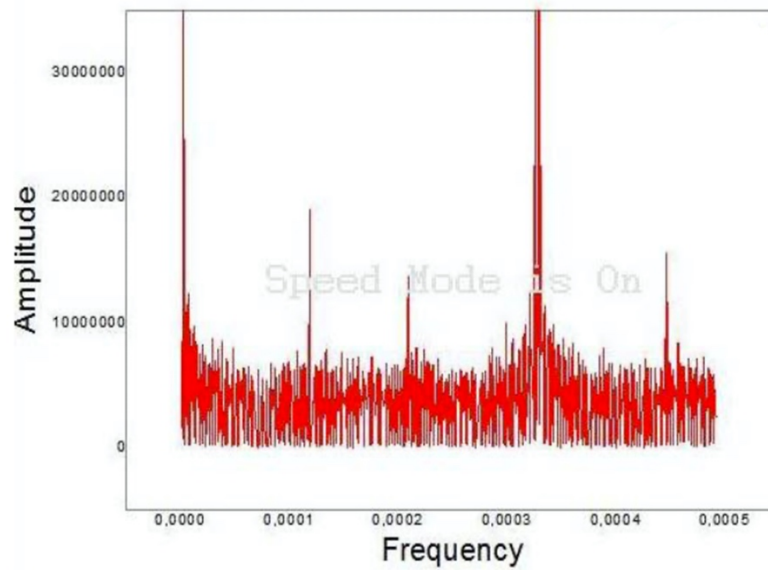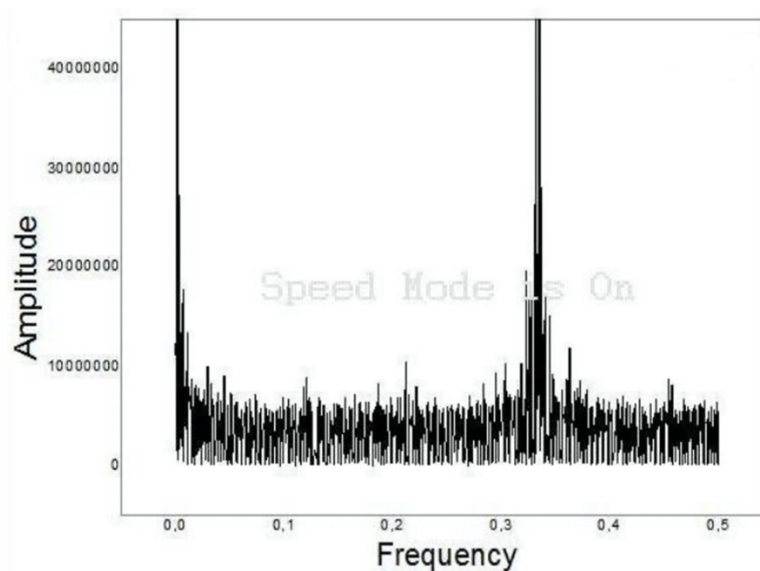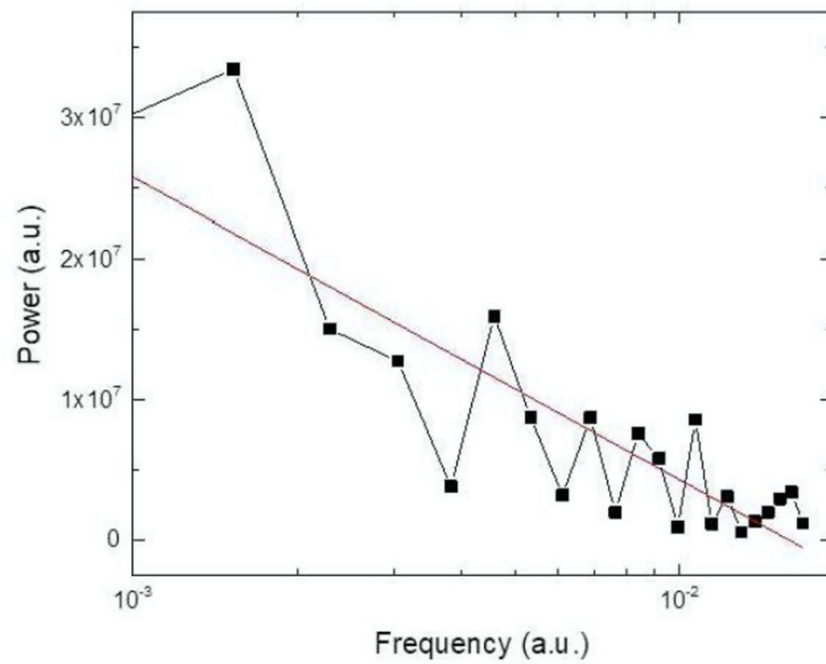
Appendix figure A1

Appendix Figure A2

C. Dal Lin and CM Radu et al." *In vitro* effects on cellular shaping, contratility, cytoskeletal organization and mitochondrial activity in HL1 cells after different sounds stimulation. A qualitative pilot study and a theoretical physical model". Figures.

Appendix Figure A3

C. Dal Lin and CM Radu et al." In vitro effects on cellular shaping, contratility, cytoskeletal organization and mitochondrial activity in HL1 cells after different sounds stimulation. A qualitative pilot study and a theoretical physical model". Figures.